Desalination and Water Treatment
www.deswater.com
doi: 10.1080/19443994.2016.1172512

57 (2016) 27259–27268
December

Taylor & Francis
Taylor & Francis Group

Removal of MTBE from aqueous solution using natural nanoclays of Iran

Najme Sadat Naser Sheykhaoleslami[a], Mohammad Irani[b,*], Romisa Gholamian[c], Majid Aliabadi[d,*]

[a]*Department of Chemistry, Islamic Azad University Saveh, Saveh Branch, Saveh, Iran, email: nsnsh_13611@yahoo.com*
[b]*Department of Chemical Engineering, Amirkabir University of Technology (Tehran Polytechnic), Tehran, Iran, email: irani_mo@ut.ac.ir*
[c]*Deputy Education, Tehran University of Medical Sciences and Health Services, Tehran, Iran, email: rGholamian@gmail.com*
[d]*Department of Chemical Engineering, Islamic Azad University, Birjand Branch, Birjand, Iran, email: m.aliabadi@iaubir.ac.ir*

Received 30 September 2015; Accepted 3 March 2016

ABSTRACT

In the present study, the adsorption capability of methyl tertiary butyl ether (MTBE) was investigated using natural nanoclays of Iran including perlite, dolomite, diatomite, and perlite/diatomite/dolomite composite. The physicochemical properties of natural clays were determined using dynamic light scattering, scanning electron microscope, Fourier Transform Inferred, X-ray fluorescence, and Brunauer–Emmet–Teller analysis. The effect of sorption parameters including contact time, initial concentration, and temperature on the MTBE removal was evaluated in a batch system. The maximum monolayer sorption capacity of nanoclays for MTBE sorption was found to be in order of: diatomite (143.19 mg g^{-1}) > perlite/diatomite/dolomite (133.12 mg g^{-1}) > dolomite (103.18 mg g^{-1}) > perlite (93.13 mg g^{-1}). The kinetic data were analyzed using pseudo-first-order and pseudo-second-order model. Freundlich, Langmuir, and Dubinin–Radushkevich isotherm models were used to describe the equilibrium data of MTBE sorption. The thermodynamic parameters (ΔG°, ΔH°, and ΔS°) indicated that the MTBE sorption using studied nanoclays was spontaneous and endothermic. The results showed that nanoclay samples due to low cost and high efficiency can be used extensively for the removal of MTBE from water in industry.

Keywords: MTBE; Diatomite; Perlite; Dolomite; Adsorption

1. Introduction

The wide use of Methyl tert-butyl ether (MTBE) as a gasoline additive leads to increase in the groundwater and surface water pollutants [1–3]. MTBE due to its high water solubility, slow biodegradability, and low Henry's law is one of the major environmental pollutants [4,5]. The presence of low amounts of MTBE is harmful to the nervous system, genotoxic, and eye irritant. The permissible limit of MTBE in water is 20–40 μg l^{-1} [6]. Therefore, the removal of MTBE from water is a very important issue with respect to human's health and environmental considerations. Various techniques including air stripping, adsorption, advanced oxidation processes, and biological treatment have been used for the removal of MTBE from aqueous systems [7]. Among techniques, the adsorption process due to its

*Corresponding authors.

simplicity, moderate operational conditions, and economic feasibility have been used as an effective method for the removal of MTBE from aqueous solutions [1]. The physicochemical properties of adsorbent play an important role in adsorption process. The high surface area and functional groups of adsorbent increase the adsorption efficiency [8]. Recently, researchers have used the porous materials including activated carbon, resins, and zeolites for the removal of MTBE from aqueous systems [2,3,9–14]. Among them, activated carbon and zeolites have been widely used for MTBE sorption with high efficiency. However, the use of them due to their high cost is limited. Therefore, it is necessary to develop the easily available, inexpensive, and an efficient material for MTBE sorption [15]. Materials, such as natural materials, rock minerals, agricultural, or industrial waste byproducts can be utilized as low-cost adsorbents. Furthermore, the nano-sized particles due to the higher specific area are more favorable for wastewater treatment compared with micro-sized particles [16]. Aivalioti et al. have investigated the performance of natural and modified diatomite with micro-size particles for MTBE sorption [15,17]. However, there is no study about the application of nanoclays for MTBE sorption from aqueous solutions.

Perlite is an excellent filter with higher content of silica. Perlite is inexpensive and abundantly available in Iran mines. The use of perlite due to the excellent chemical property and easily availability has been considered as an economical adsorbent for the removal of water pollutants [18,19].

Dolomite with the formula [$CaMg(CO_3)_2$] as a low-cost adsorbent is used for the removal of heavy metal ions [20–23]. Miyaneh area has the main source of dolomite in Iran.

Diatomite consists of amorphous silica ($SiO_2{\cdot}nH_2O$) matrix. Diatomite due to its high permeability and porosity as well as high surface area has been widely used for the removal of different elements from water and wastewaters [24]. Kamelabad area of Iran has the main source of diatomite. The cost of diatomite, perlite, and dolomite is less than 12, 14, and 8 $ per ton in Iran.

In this work, diatomite, perlite, dolomite, and perlite/diatomite/dolomite composite nanoparticles were provided from Iran mines. The prepared nanoparticles were characterized using dynamic light scattering (DLS), scanning electron microscope (SEM), X-ray fluorescence (XRF), and Brunauer–Emmet–Teller (BET) analysis. The nature of the adsorption process with respect to its kinetics, isotherms, and thermodynamic aspects has been also evaluated.

2. Experiments

2.1. Materials

The row diatomite, perlite, and dolomite were provided from Kamelabad, Oshlogh Chay, and Miyaneh mines of Iran, respectively. At first, natural clay particles were washed by distilled water to remove impurities, and were dried at 110°C for 8 h. Then, dried samples were powdered in a ball mill consisting of distilled water in 250 rpm for 5 h. Finally, slurry samples were dehumidified using spray dryer in 140°C according to the previous study [25]. The prepared nanoclays were used in adsorption process. The perlite/diatomite/dolomite composite was prepared with the equal ratio of perlite, diatomite, and dolomite. The chemical composition of prepared clay nanoparticles was determined by XRF analysis and the results are listed in Table 1.

MTBE (purity >99%) was purchased from Merck (Germany). The MTBE standards were prepared using distilled water.

2.2. Characterization tests

The functional groups of clay samples were determined by a Fourier Transform Inferred Spectrometer (Vector22-Bruker Company, Germany) in the range of 400–4,000 cm^{-1}. The morphology of nanoclays was characterized using a scanning electron microscope (SEM, JEOL JSM-6380) after gold coating. The XRF (Philips instrument) was used to evaluate the elemental compositions of clays. The size distribution of the clay nanoparticles was determined using DLS analysis (Malvern Instruments, Worcestershire). The average pore diameter, specific surface area, and pore volume of the prepared clay nanoparticles were measured by the BET method. For determination of the point of the zero charge (pH_{pzc}) of nanoclays, 50 mL of 0.1 M NaCl was transferred in series of flasks. The solutions pH was adjusted in the range 2–7 by adding 0.1 M HNO_3 or/and 0.1 M NaOH solutions. Then, 0.2 g adsorbent was added into the solution. After that, the solutions were shaken for 5 days at 25°C. Finally, the pH of the solutions was measured. pH_{pzc} was reported at the pH in which the initial pH equals the final pH [8].

The final concentration of MTBE was determined using gas chromatography/mass spectrometry system (Varian BV, Austria) equipped with a capillary column (50 m × 0.25 mm × 1 μm). Carrier gas was helium with a flow rate of 1 mL min^{-1}. The split ratio was 1:20. The oven temperatures were 30°C initially for 12 min and then ramp to 170°C by the rate of 30°C min^{-1}. The injector temperature was 200°C.

Table 1
Chemical composition of perlite, dolomite, and diatomite

Component	Perlite (wt%)	Dolomite (wt%)	Diatomite (wt%)	Perlite/dolomite/diatomite (wt%)
SiO_2	73.32	0.41	89.20	60.30
Al_2O_3	12.62	0.12	4.10	5.21
K_2O	5.02	2.10	0.63	2.30
Na_2O	2.96	0.71	1.21	1.34
Cao	0.66	31.69	0.50	11.23
Fe_2O_3	0.67	0.26	1.50	1.02
MnO	0.66	–	–	0.30
MgO	0.21	23.64	0.30	9.21
P_2O_5	0.13	0.11	0.11	0.11
SO_3	–	0.03	–	0.03
L.O.I	3.75	40.93	2.45	8.95

2.3. Batch adsorption experiments

The performance of prepared nanoclay adsorbents for MTBE ions sorption was investigated as a function of contact time (0–180 min), initial concentration (20–500 mg L^{-1}), and temperature (298–318 K) in a batch system. For this, 100 mg of nanoparticles were placed in a flask containing 10 mg L^{-1} of MTBE solution on a rotary shaker at 200 rpm for 2 h. The pH of MTBE solution was adjusted at pH of 5.2 by adding 0.1 M HCl or/and 0.1 M NaOH solutions. Each experiment was repeated triplicate and the results were given as averages. The amount of the MTBE adsorbed was calculated as follows:

$$q_e = \frac{(C_0 - C_e)V}{1000\,M} \quad (1)$$

where q_e is the adsorption capacity in mg g^{-1}, C_0 and C_e are the initial and equilibrium concentrations of MTBE in mg L^{-1}, V is the volume of the solution in mL, and M is the weight of the dry absorbent in g.

3. Results and discussion

3.1. Characterization of nanoclays

DLS analysis was performed to evaluate the particle size distribution of four clay samples including diatomite, dolomite, perlite, and perlite/diatomite/dolomite nanoclays. Results are presented in Fig. 1 as shown, the average particle sizes of diatomite, perlite/diatomite/dolomite, dolomite, and perlite clays were found to be 56, 79, 110, and 132 nm, respectively. Also, the results demonstrated that the diatomite nanoclays had much narrower size distribution compared with other synthesized clay samples.

The SEM images of clay samples are illustrated in Fig. 2. As shown, the diatomite nanoparticles were

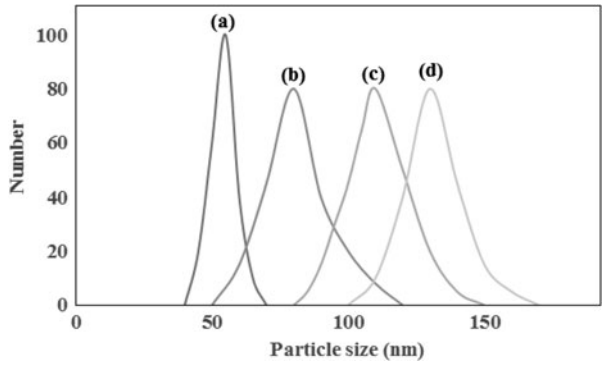

Fig. 1. DLS of (a) diatomite, (b) perlite/diatomite/dolomite, (c) dolomite, and (d) perlite.

successfully synthesized with smaller sizes with no agglomeration of particles and the particle size distribution of diatomite was more uniform compared with other synthesized clay samples. Whereas, the agglomeration of particles was observed for perlite/diatomite/dolomite, dolomite, and perlite clays.

The Fourier Transform Inferred (FTIR) spectra of diatomite, dolomite, and perlite are illustrated in Fig. 3. The peak at 3,620 cm^{-1} band of diatomite nanoparticles was attributed to the OH vibration. The peaks of Si–OH and/or Al–OH were found at 920 cm^{-1} and the peak at 530 cm^{-1} was assigned to the Si–O–Al band in the diatomite structure. The broad band between 3,750 and 3,000 cm^{-1} was attributed to the vibration of hydroxyl groups at the perlite surface. The bands at 800–1,250 cm^{-1} were assigned to the Si–O vibrations and the Al–OH–Al or Al–OH–Mg groups of perlite were found at about 850–900 cm^{-1}. The absorption bands of dolomite were observed at 3,420, 1,440, 880, and 730 cm^{-1}. The peak at around 3,420 was due to the O–H stretching for the hydrogen

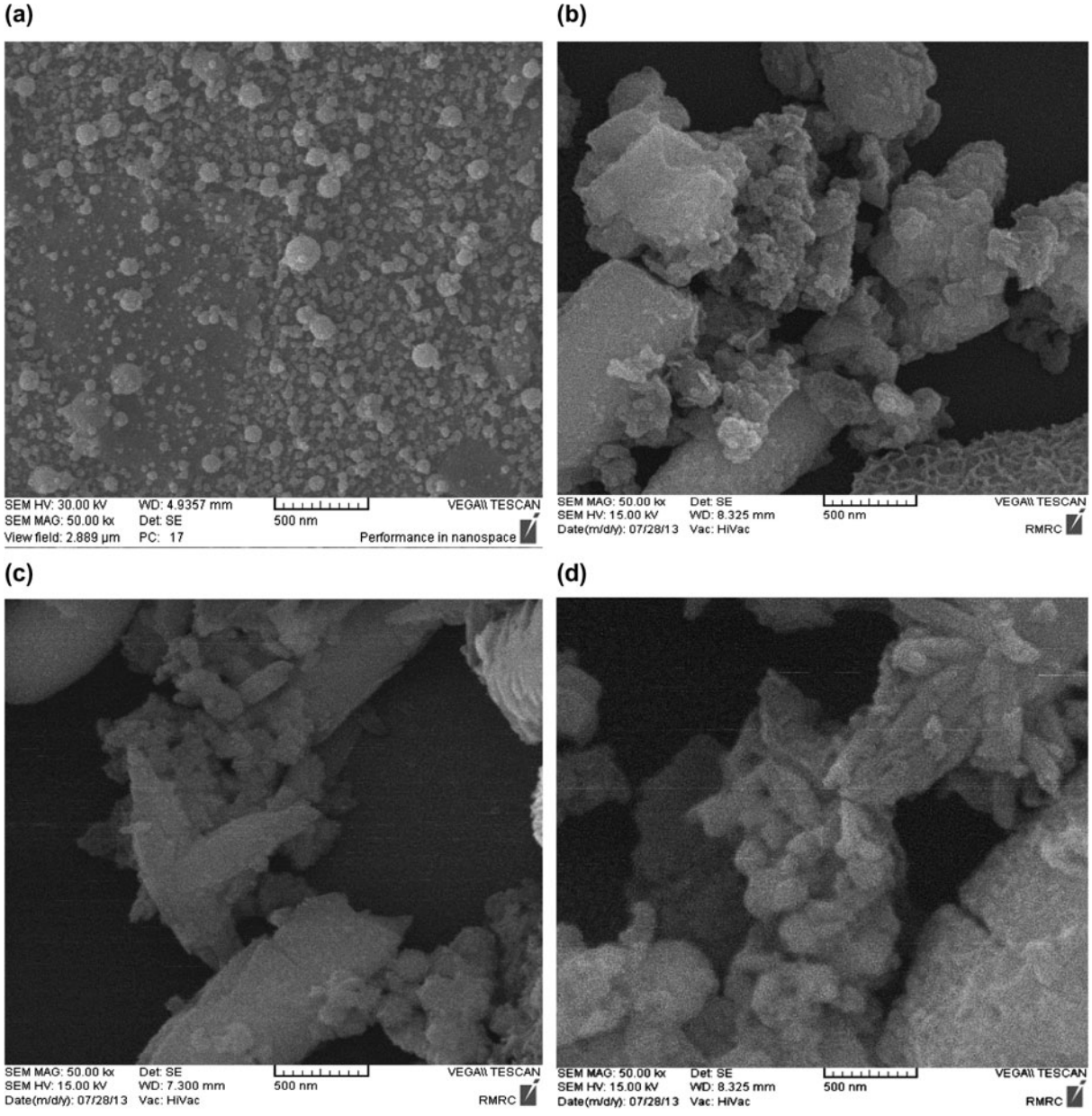

Fig. 2. SEM images of (a) diatomite, (b) perlite/diatomite/dolomite, (c) dolomite, and (d) perlite.

bonded hydroxyl groups. The carbonate group peak was observed around 1,440 cm^{-1}. The Mg–O or/and Ca–O groups were seen at 729 and 880 cm^{-1}.

The point of the zero charge of diatomite, perlite/diatomite/dolomite, dolomite, and perlite was found to be 3.6, 3.8, 3.9, and 4.3, respectively.

Based on BJH theory, the average pore diameter, the BET surface area (S_{BET}), and the pore volume of clay samples are listed in Table 2. Based on results, the S_{BET} of diatomite, perlite/diatomite/dolomite, dolomite, and perlite clays was found to be 119.3, 98.7, 72.6, and 59.2 $m^2\ g^{-1}$, respectively.

3.2. Effect of contact time on the MTBE sorption

The influence of contact time on the removal of MTBE in initial concentration of 20 mg L^{-1}, adsorbent dosage of 1 g L^{-1}, pH of 5.2, and temperature of 25°C is illustrated in Fig. 4. As shown, more than 95% of the total adsorption of MTBE was occurred within 90 min and after 120 min, MTBE sorption using nanoclays did not change significantly with operation time.

Therefore, the equilibrium time of 120 min was selected as an equilibrium time for further experiments.

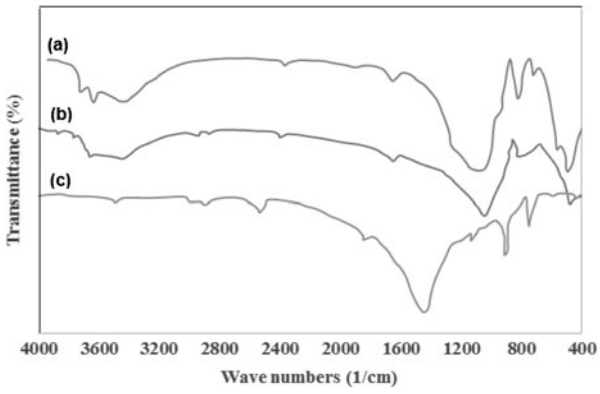

Fig. 3. FTIR spectra of (a) diatomite, (b) perlite, and (c) dolomite.

Also, the smaller sizes of diatomite particles with narrower particle size distribution, higher surface area, and more functional groups of diatomite led to the more available active sites for MTBE sorption compared with other studied nanoclay samples.

Kinetic models, namely pseudo-first-order and pseudo-second-order models were used to describe the adsorption kinetics of MTBE into the clay samples.

The pseudo-first-order kinetic model by Lagergren [26] is given as follows:

$$q_t = q_e(1 - \exp(-k_1 t)) \tag{2}$$

The pseudo-second-order kinetic model by Ho and Mc Kay [27] is given as follows:

$$q_t = \frac{k_2 q_e^2 t}{1 + k_2 q_e t} \tag{3}$$

where q_t and q_e (mg g^{-1}) are the adsorption capacity at time t and equilibrium time. k_1 (min^{-1}) and k_2 (g mg^{-1} min^{-1}) are the pseudo-first-order and pseudo-second-order models constants. The results are presented in Table 3. By contrasting the correlation coefficients for pseudo-first-order ($R^2 > 0.976$) and pseudo-second-order ($R^2 > 0.995$), it was found that the kinetic data of MTBE by nanoclay samples were well described by pseudo-second-order model compared with pseudo-first-order model.

3.3. Effect of initial concentration and isotherm models

The influence of MTBE initial concentration by the clay samples on the adsorption process at different temperatures (25, 35, and 45°C) is illustrated in Fig. 5. As shown, the MTBE sorption capacity was increased by increasing MTBE concentration and was then approached a fixed value.

The increase in the sorption capacity of MTBE could be attributed to the increase in the driving force gradient for mass transfer created by the increase in initial concentration. The fixed value of the adsorption capacity was attributed to the saturation of the active available sites of the clay samples. Furthermore, the sorption capacity of MTBE was favorable at higher temperature which indicated the endothermic nature of sorption process using the studied nanoclay samples.

The known isotherm models including Freundlich, Langmuir, and Dubinin–Radushkevich (D–R) were applied to describe the equilibrium data of MTBE sorption by the clay samples. The parameters of isotherm models were calculated by nonlinear regression of q_e vs. C_e using MATLAB software. The results are listed Table 4.

The Freundlich isotherm equation is expressed as follows [28]:

$$q_e = k_F C_e^{\frac{1}{n}} \tag{4}$$

The Langmuir isotherm model [29] is expressed as follows:

$$q_e = q_m \frac{bC_e}{1 + bC_e} \tag{5}$$

where k_F (mg g^{-1}) and n are Freundlich parameters related to the sorption capacity and intensity of the

Table 2
Physical properties of studied nanoclay adsorbents

Sample	SBET (m^2 g^{-1})	Pore volume (cm^3 g^{-1})	Average pore diameter (nm)
Perlite	59.2	0.103	1.40
Dolomite	72.6	0.129	1.54
Diatomite	119.3	0.187	2.12
Perlite/dolomite/diatomite	98.7	0.157	1.89

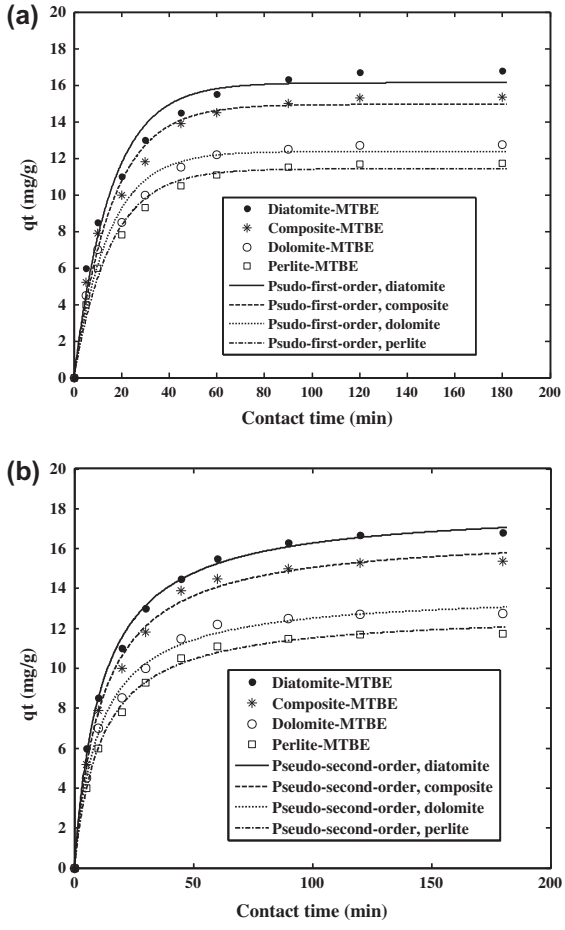

Fig. 4. (a) pseudo-first-order and (b) pseudo-second-order kinetics of MTBE sorption onto the diatomite, perlite/diatomite/dolomite composite, dolomite, and perlite.

sorbent, respectively. q_{max} (mg g^{-1}) and b (m g^{-1}) are the Langmuir model constants.

q_m is the maximum value of MTBE adsorption per unit weight of adsorbent that is related to the monolayer adsorption capacity and b is related to the enthalpy of adsorption.

The D–R isotherm model was also used to determine the physical or chemical nature of adsorption processes. The D–R isotherm model is expressed as follows [30]:

$$q_e = q_{DR} \exp(-B_{DR}\varepsilon_{DR}^2) \quad (6)$$

where q_e is the mole amount of metal ions adsorbed on per unit weight of biomass (mmol g^{-1}), q_{DR} is the maximum adsorption capacity (mmol g^{-1}), β is the activity coefficient related to adsorption mean free energy (mol^2 J^{-2}), and ε is the polanyi potential ($\varepsilon = RT \ln(1 + 1/C_{eq})$), R is the gas constant (8.314 J mol^{-1} K^{-1}), and T is the absolute temperature (K). The Polanyi sorption theory assumes a fixed volume of sorption space close to the sorbent surface and the existence of a sorption potential over these spaces. The mean free energy of adsorption (E, J mol^{-1}) can be calculated from the following equation:

$$E = \frac{1}{\sqrt{2\beta}} \quad (7)$$

The free energy of adsorption gives information about physical or chemical adsorption mechanism. If the free energy is greater than 8 kJ mol^{-1}, the adsorption process takes place chemically and while $E < 8$ kJ mol^{-1}, the adsorption process proceeds physically [31,32]. As shown in Table 4, the adsorption free energy was calculated from 3.40 to 4.30, 3.21 to 4.05, 2.80 to 3.25, and 1.80 to 2.60 kJ mol^{-1} by increasing temperature from 25 to 45°C for adsorption of MTBE from aqueous solution using diatomite, perlite/diatomite/dolomite, dolomite, and perlite. These results indicated that the mechanism of MTBE sorption onto the studied clays was physical adsorption.

By comparing the correlation coefficients, it was found that the equilibrium data of MTBE were best described by Langmuir isotherm model ($R^2 > 0.990$) compared with Freundlich ($R^2 > 0.952$) and D–R ($R^2 > 0.935$) isotherm model. The obtained results demonstrated the monolayer sorption mechanism of MTBE onto the studied clay samples.

Table 3
Kinetic parameters of MTBE sorption onto the clay samples

	Pseudo-first-order model			Pseudo-second-order model		
Adsorbent	q_{eq} (mg g^{-1})	K_1 (min^{-1})	R^2	q_{eq}	K_2 (g mg^{-1} min^{-1})	R^2
Diatomite	16.13	0.0649	0.976	18.13	0.00485	0.997
Composite	14.95	0.0634	0.982	16.80	0.00510	0.995
Dolomite	12.37	0.0689	0.981	13.83	0.00686	0.995
Perlite	11.42	0.0652	0.985	12.83	0.00685	0.996

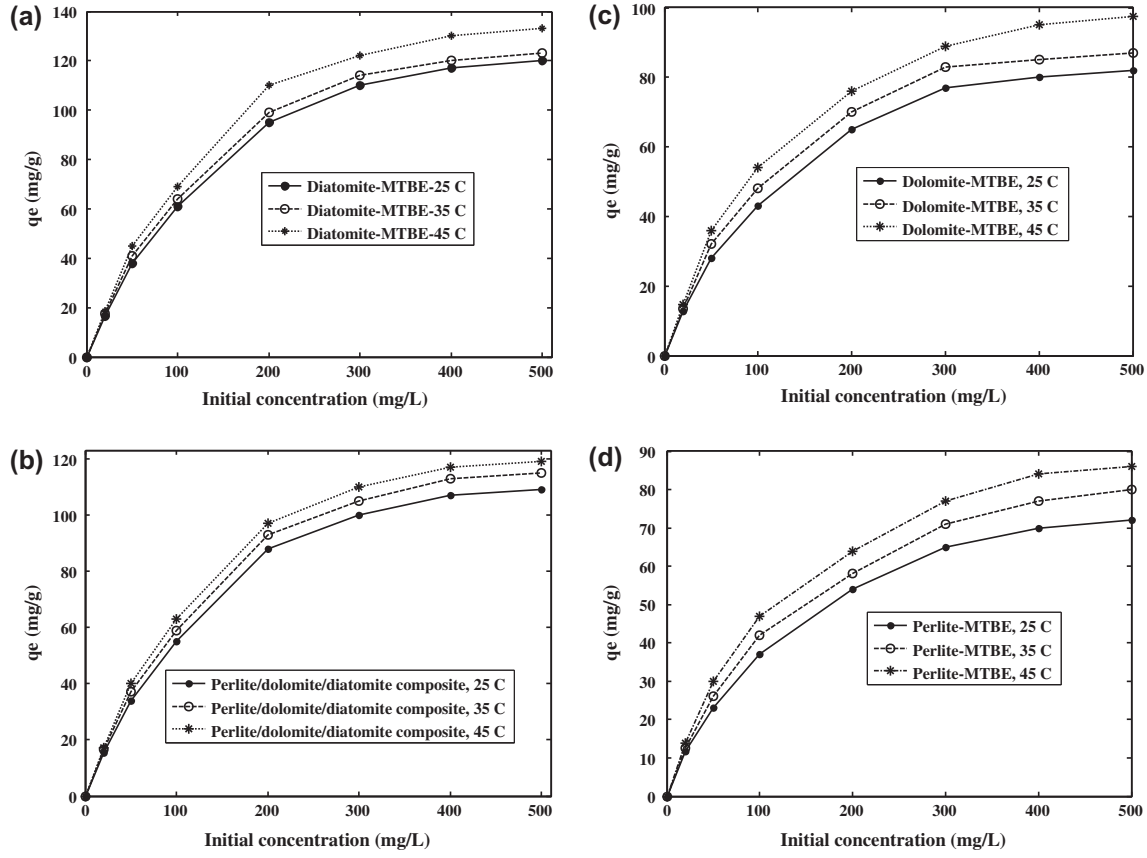

Fig. 5. Effect of initial concentration of MTBE on the sorption capacity of (a) diatomite, (b) perlite/diatomite/dolomite composite, (c) dolomite, and (d) perlite.

Table 4
Isotherm parameters of MTBE sorption onto the clay samples

		Freundlich isotherm			Langmuir isotherm			D–R isotherm			
Adsorbent	T (°C)	K_F (mg g^{-1})	n	R^2	q_{max} (mg g^{-1})	K_L (L mg^{-1})	R^2	q_{DR} (mmol g^{-1})	B_{DR} ((mol^2 J^2)$^{-1}$)	E (kJ mol^{-1})	R^2
Diatomite	25	25.69	3.823	0.965	128.26	0.04211	0.990	1.27	4.326×10^{-8}	3.40	0.952
	35	28.42	4.196	0.953	132.94	0.05081	0.991	1.32	3.304×10^{-8}	3.89	0.956
	45	30.37	4.320	0.957	143.19	0.06101	0.993	1.42	2.704×10^{-8}	4.30	0.962
Composite	25	23.67	3.665	0.971	120.06	0.04211	0.989	1.15	4.852×10^{-8}	3.21	0.935
	35	25.59	3.974	0.963	126.94	0.04781	0.993	1.21	3.537×10^{-8}	3.76	0.942
	45	27.90	4.126	0.969	133.12	0.05101	0.992	1.28	3.048×10^{-8}	4.05	0.950
Dolomite	25	17.67	3.865	0.975	89.06	0.03411	0.993	0.88	6.378×10^{-8}	2.80	0.951
	35	21.59	4.196	0.963	95.94	0.03781	0.992	0.95	5.482×10^{-8}	3.02	0.956
	45	24.90	4.220	0.952	103.18	0.04101	0.994	1.03	4.734×10^{-8}	3.25	0.960
Perlite	25	15.27	3.475	0.975	75.06	0.03071	0.990	0.73	1.543×10^{-7}	1.80	0.945
	35	17.13	3.676	0.963	85.94	0.03225	0.991	0.84	1.005×10^{-7}	2.23	0.949
	45	19.01	4.050	0.952	93.13	0.03548	0.992	0.92	7.396×10^{-8}	2.60	0.952

3.4. Adsorption mechanism

By considering the MTBE ionization in water ($MTBE \rightarrow MTBE^{+} + OH^{-}$), the possible mechanisms influencing the MTBE sorption between the MTBE molecules and clay samples were (1) the electrostatic attraction between the positively charge of MTBE and negative charge of clay samples (such as hydroxyl) and (2) the adsorption on the surface adsorbents which the higher surface area could be responsible for more MTBE sorption.

3.5. Thermodynamic parameters

The Gibbs free energy change (ΔG°) of thermodynamic parameters for MTBE sorption by the nanoclay samples were evaluated by the following equations:

$$k_C = \lim_{C_{el} \to 0} \frac{C_{es}}{C_{el}} \tag{8}$$

$$\Delta G^{\circ} = -RT \ln k_C \tag{9}$$

where C_{es} and C_{el} are the values of solid and liquid phase concentration in equilibrium (mg L^{-1}), respectively. R (kJ mol^{-1} K^{-1}) is the gas constant, T (K) is the temperature, and k_C is the adsorption equilibrium constant. The entropy change (ΔS°) and enthalpy change (ΔH°) were determined from the Van't Hoff equation as follows:

$$\ln k_C = \frac{\Delta S^{\circ}}{R} - \frac{\Delta H^{\circ}}{RT} \tag{10}$$

ΔH° and ΔS° were obtained from the slope and intercept of $\ln k_C$ vs. $1/T$ plot (Fig. 6).

The results are listed in Table 5. The negative values of ΔG° indicated the spontaneous nature of the MTBE sorption onto the clay samples. The positive values of ΔH° showed the endothermic mechanism of the MTBE sorption and more affinity of clay samples for MTBE sorption at higher temperatures. The positive value of ΔS° showed that the randomness was increased at the solid-solution interface.

3.6. Comparison study

Activated carbon has been widely studied for adsorption of MTBE from water. Granular activated carbon (GAC) was tested for MTBE adsorption and the maximum adsorption capacity was reported to be 204.1 mg g^{-1} at GAC concentration of 1 g L^{-1} [9].

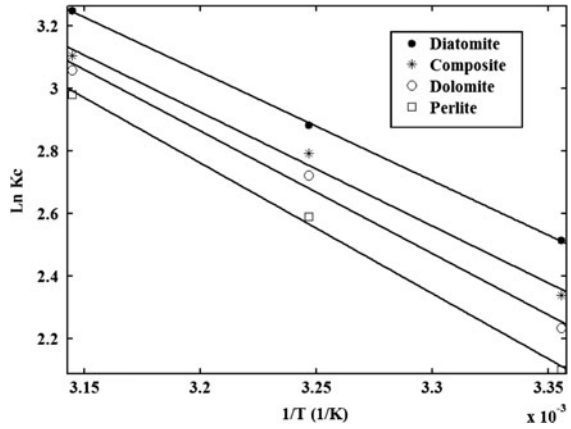

Fig. 6. Linear plot of $\ln k_c$ vs. $1/T$ for evaluation of ΔH° and ΔS°.

Zeolites are microporous alumosilicate minerals commonly used as commercial adsorbents for pollutant removal from water and wastewater. Anderson investigated the potential of high silica containing zeolites for MTBE and other organic contaminant removal. Efficiency of tested sorbents for removal of MTBE with concentration 100 μg L^{-1} from water was shown in order: mordenite (96%) > ZSM-5 (63%) > activated carbon (52%) > Y (5%) [33]. Abu-Lail et al. [3] tested for adsorption of MTBE in the range 10–100 mg L^{-1} using zeolites, coconut shell GAC (CS-1240), and commercial carbon adsorbents. The obtained results indicated that the ZSM-5 adsorbent showed higher sorption capacity among all the tested zeolites at studied condition. The performance of zeolite composites (silicalite/fly ash and silicalite/diatomite) was examined in the range 0.1–1 mg L^{-1}. Silicalite/fly ash had a higher maximum adsorption capacity (q_{max} = 92.55 mg g^{-1}) than silicalite/diatomite (q_{max} = 48.46 mg g^{-1}). However, the use of zeolites due to their high cost was limited.

A few studies have been published recently for MTBE removal from water using resins. The monolayer sorption affinity for MTBE and TBA was found to be in the order: Ambersorb 563 > L493 > XAD4 > XAD7 [34].

The maximum monolayer adsorption capacities of diatomite, perlite/diatomite/dolomite, dolomite, and perlite nanoclays were found to be 143.19, 133.12, 103.18, and 93.13 mg g^{-1}. As shown, the sorption capacity of nanoclay samples for MTBE removal was found to be comparable and moderately higher than those of many corresponding sorbents. Also, diatomite nanoparticles had a significant potential for MTBE sorption compared with other studied clay samples. It could be attributed to the higher surface area of diatomite nanoparticles compared with perlite and dolomite.

Table 5
Thermodynamic parameters of MTBE sorption onto the clay samples

Adsorbent	k_C			ΔH° (kJ mol^{-1})	ΔS° (kJ mol K^{-1})	ΔG° (kJ mol^{-1})		
	25℃	35℃	45℃			25℃	35℃	45℃
Diatomite	12.35	17.89	25.80	29.016	0.118	−6.228	−7.386	−8.594
Composite	10.36	16.33	22.34	30.321	0.121	−5.792	−7.152	−8.213
Dolomite	9.33	15.21	21.34	32.641	0.129	−5.533	−6.970	−8.092
Perlite	8.16	13.33	19.70	34.753	0.134	−5.201	−6.632	−7.880

4. Conclusion

In this work, the performance of perlite, dolomite, diatomite, and perlite/diatomite/dolomite composite nanoclays provided from Iran mines was investigated for MTBE sorption from aqueous solutions. DLS indicated that the average particle size of diatomite, perlite/diatomite/dolomite, dolomite, and perlite clays was 56, 79, 110, and 150 nm, respectively.

The kinetic data of MTBE were well described by pseudo-second-order model at equilibrium time of 120 min. The MTBE equilibrium data followed well the Langmuir isotherm model with maximum monolayer sorption capacity of 143.19, 133.12, 103.18, and 93.13 mg g^{-1} using diatomite, perlite/diatomite/dolomite, dolomite, and perlite clays at temperature of 45℃. The investigation of free energy of adsorption from the D–R isotherm model indicated that the mechanism of MTBE sorption onto the studied clays was physical adsorption. The obtained thermodynamic parameters indicated the spontaneous and endothermic nature of MTBE sorption onto the studied nanoclay adsorbents. The obtained results confirmed that the studied nanoclay samples as low-cost adsorbents can be widely utilized for the removal of MTBE from water.

References

[1] F.E. Ahmed, Toxicology and human health effects following exposure to oxygenated or reformulated gasoline, Toxicol. Lett. 123 (2001) 89–113.
[2] B. Ji, F. Shao, G. Hu, S. Zheng, Q. Zhang, Z. Xu, Adsorption of methyl *tert*-butyl ether (MTBE) from aqueous solution by porous polymeric adsorbents, J. Hazard. Mater. 161 (2009) 81–87.
[3] L.A. Laila, J.A. Bergendahl, R.W. Thompson, Adsorption of methyl tertiary butyl ether on granular zeolites: Batch and column studies, J. Hazard. Mater. 178 (2010) 363–369.
[4] R.W. Gullick, M.W. LeChevallier, Occurrence of MTBE in drinkingwater sources, J. AWWA 92 (2000) 100–113.
[5] H.W. Hung, T.F. Lin, Adsorption of MTBE from contaminated water by carbonaceous resins and mordenite zeolite, J. Hazard. Mater. 135 (2006) 210–217.
[6] USEPA, Drinking Water Advisory: Consumer Acceptability Advice and Health Effects Analysis on Methyl Tertiary-Butyl Ether (MTBE), 1997.
[7] I. Levchuk, A. Bhatnagar, M. Sillanpää, Overview of technologies for removal of methyl tert-butyl ether (MTBE) from water, Sci. Total Environ. 476–477 (2014) 415–433.
[8] M. Irani, M. Amjadi, M.A. Mousavian, Comparative study of lead sorption onto natural perlite, dolomite and diatomite, Chem. Eng. J. 178 (2011) 317–323.
[9] D.Z. Chen, J.X. Zhang, J.M. Chen, Adsorption of methyl tert-butyl ether using granular activated carbon: Equilibrium and kinetic analysis, Int. J. Environ. Sci. Technol. 7 (2010) 235–242.
[10] F. Inal, S. Yetgin, G.T. Aksu, S. Simsek, A. Sofuoglu, S.C. Sofuoglu, Activated carbon adsorption of fuel oxygenates MTBE and ETBE from water, Water Air Soil Pollut. 204 (2009) 155–163.
[11] A. Rossner, D.R.U. Knappe, MTBE adsorption on alternative adsorbents and packed bed adsorber performance, Water Res. 42 (2008) 2287–2299.
[12] R. Arletti, A. Martucci, A. Alberti, L. Pasti, M. Nassi, R. Bagatin, Location of MTBE and toluene in the channel system of the zeolite mordenite: Adsorption and host–guest interactions, J. Solid State Chem. 194 (2012) 135–142.
[13] B. Burghoff, J.S. Marques, B.M. van Lankvelt, A.B. de Haan, Solvent impregnated resins for MTBE removal from aqueous environments, React. Funct. Polym. 70 (2010) 41–47.
[14] S.K. Ghadiri, R. Nabizadeh, A.H. Mahvi, S. Nasseri, A.R. Mesdaghinia, S.S. Talebi, Potential of granulated modified nanozeolites Y for MTBE removal from aqueous solutions: Kinetic and isotherm studies, Polish J. Chem. Technol. 14 (2012) 1–8.
[15] M. Aivalioti, I. Vamvasakis, E. Gidarakos, BTEX and MTBE adsorption onto raw and thermally modified diatomite, J. Hazard. Mater. 178 (2010) 136–143.
[16] J. Lu, F. Xu, W. Cai, Adsorption of MTBE on nano zeolite composites of selective supports, Microporous Mesoporous Mater. 108 (2008) 50–55.
[17] M. Aivalioti, P. Papoulias, A. Kousaiti, E. Gidarakos, Adsorption of BTEX, MTBE and TAME on natural and modified diatomite, J. Hazard. Mater. 207–208 (2012) 117–127.
[18] T. Mathialagan, T. Viraraghavan, Adsorption of cadmium from aqueous solutions by perlite, J. Hazard. Mater. 94 (2002) 291–303.
[19] M. Torab-Mostaedi, A. Ghaemi, H. Ghassabzadeh, M. Ghannadi-Maragheh, Removal of strontium and

barium from aqueous solutions by adsorption onto expanded perlite, Can. J. Chem. Eng. 89 (2011) 1247–1254.
[20] E. Pehlivan, A.M. Özkan, S. Dinç, Ş. Parlayici, Adsorption of Cu^{2+} and Pb^{2+} ion on dolomite powder, J. Hazard. Mater. 167 (2009) 1044–1049.
[21] A. Ghaemi, M. Torab Mostaedi, M. M. Ghannadi-Maragheh, Characterizations of strontium(II) and barium (II) adsorption from aqueous solutions using dolomite powder. J. Hazard. Mater. 190(2011) 916–921.
[22] A. Ghaemi, M. Torab-Mostaedi, S. Shahhosseini, M. Asadollahzadeh, Characterization of Ag(I), Co(II) and Cu (II) removal process from aqueous solutions using dolomite powder, Korean J. Chem. Eng. 30 (2013) 172–180.
[23] M. Mohammadi, A. Ghaemi, M. Torab Mostaedi, Adsorption of cadmium and nickel from aqueous solutions using dolomite powder, Desalin. Water Treat. 53 (2015), 149–157.
[24] M. Al-Ghouti, M.A.M. Khraisheh, M.N. Ahmad, S. Allen, Thermodynamic behaviour and the effect of temperature on the removal of dyes from aqueous solution using modified diatomite: A kinetic study, J. Colloid Interface Sci. 287 (2005) 6–13.
[25] H. Beheshti, M. Irani, Removal of lead(II) ions from aqueous solutions using diatomite nanoparticles, Desalin. Water Treat. doi: 10.1080/19443994.2015.1095683
[26] S. Lagergren, Zur theorie der sogenannten adsorption geloster stoffe (About the theory of so-called adsorption of soluble substances), Kung-liga Sevenska Vetenskapsakademiens Handlingar 24 (1898) 1–39.
[27] Y.S. Ho, G. McKay, Pseudo-second-order model for sorption processes, Process Biochem. 34 (1999) 451–465.
[28] H.M.F. Freundlich, Uber die adsorption in losungen (Over the adsorption in solution), J. Phys. Chem. 57 (1906) 385–470.
[29] I. Langmuir, The constitution and fundamental properties of solids and liquids, J. Am. Chem. Soc. 38 (1916) 2221–2295.
[30] M.M. Dubinin, E.D. Zaverina, L.V. Radushkevich, Sorption and structure of active carbons. I. Adsorption of organic vapors, Zhurnal Fizicheskoi Khimii 21 (1947) 1351–1362.
[31] A.R. Keshtkar, M. Irani, M.A. Moosavian, Removal of uranium (VI) from aqueous solutions by adsorption using a novel electrospun PVA/TEOS/APTES hybrid nanofiber membrane: Comparison with casting PVA/TEOS/APTES hybrid membrane, J. Radioanal. Nucl. Chem. 295 (2013) 563–571.
[32] M. Irani, A.R. Keshtkar, M.A. Mousavian, Removal of Cd(II) and Ni(II) from aqueous solution by PVA/TEOS/TMPTMS hybrid membrane, Chem. Eng. J. 175 (2011) 251–259.
[33] M.A. Anderson, Removal of MTBE and other organic contaminants from water by sorption to high silica zeolites, Environ. Sci. Technol. 34 (2000) 725–727.
[34] A. Mirzaei, A. Ebadi, P. Khajavi, Kinetic and equilibrium modeling of single and binary adsorption of methyl tert-butyl ether (MTBE) and tert-butyl alcohol (TBA) onto nano-perfluorooctyl alumina, Chem. Eng. J. 231 (2013) 550–560.